

RESEARCH ARTICLE

The *FgNot3* Subunit of the Ccr4-Not Complex Regulates Vegetative Growth, Sporulation, and Virulence in *Fusarium graminearum*

Duc-Cuong Bui¹, Hokyoung Son^{1,2}, Ji Young Shin¹, Jin-Cheol Kim³, Hun Kim⁴, Gyung Ja Choi⁴, Yin-Won Lee^{1*}

1 Department of Agricultural Biotechnology and Center for Fungal Pathogenesis, Seoul National University, Seoul, Republic of Korea, **2** Center for Food and Bioconvergence, Seoul National University, Seoul, Republic of Korea, **3** Division of Applied Bioscience and Biotechnology, Institute of Environmentally Friendly Agriculture, College of Agriculture and Life Sciences, Chonnam National University, Gwangju, Republic of Korea, **4** Eco-friendly New Materials Research Group, Research Center for Biobased Chemistry, Division of Convergence Chemistry, Korea Research Institute of Chemical Technology, Daejeon, Republic of Korea

* lee2443@snu.ac.kr



OPEN ACCESS

Citation: Bui D-C, Son H, Shin JY, Kim J-C, Kim H, Choi GJ, et al. (2016) The *FgNot3* Subunit of the Ccr4-Not Complex Regulates Vegetative Growth, Sporulation, and Virulence in *Fusarium graminearum*. PLoS ONE 11(1): e0147481. doi:10.1371/journal.pone.0147481

Editor: Jae-Hyuk Yu, The University of Wisconsin - Madison, UNITED STATES

Received: November 12, 2015

Accepted: January 5, 2016

Published: January 22, 2016

Copyright: © 2016 Bui et al. This is an open access article distributed under the terms of the [Creative Commons Attribution License](https://creativecommons.org/licenses/by/4.0/), which permits unrestricted use, distribution, and reproduction in any medium, provided the original author and source are credited.

Data Availability Statement: All relevant data are within the paper and its Supporting Information files.

Funding: This work was supported by a National Research Foundation of Korea (NRF) grant funded by the Korean government (2013R1A6A3A04059121) and the Cooperative Research Program for Agricultural Science and Technology Development (Project PJ01085602), Rural Development Administration, Republic of Korea. The funders had no role in study design, data collection and analysis, decision to publish, or preparation of the manuscript.

Abstract

The Ccr4-Not complex is evolutionarily conserved and important for multiple cellular functions in eukaryotic cells. In this study, the biological roles of the *FgNot3* subunit of this complex were investigated in the plant pathogenic fungus *Fusarium graminearum*. Deletion of *FgNOT3* resulted in retarded vegetative growth, retarded spore germination, swollen hyphae, and hyper-branching. The $\Delta Fgnot3$ mutants also showed impaired sexual and asexual sporulation, decreased virulence, and reduced expression of genes related to conidiogenesis. *Fgnot3* deletion mutants were sensitive to thermal stress, whereas *NOT3* orthologs in other model eukaryotes are known to be required for cell wall integrity. We found that *FgNot3* functions as a negative regulator of the production of secondary metabolites, including trichothecenes and zearalenone. Further functional characterization of other components of the Not module of the Ccr4-Not complex demonstrated that the module is conserved. Each subunit primarily functions within the context of a complex and might have distinct roles outside of the complex in *F. graminearum*. This is the first study to functionally characterize the Not module in filamentous fungi and provides novel insights into signal transduction pathways in fungal development.

Introduction

Fusarium graminearum is an ascomycetous fungus that causes *Fusarium* head blight in cereal crops worldwide, including wheat, barley, and rice, as well as ear and stalk rot in maize [1, 2]. Fungal infection of *F. graminearum* leads to yield and quality losses as well as contamination of grains by the production of mycotoxins (trichothecenes and zearalenone) that threaten human and animal health [3]. *F. graminearum* produces both sexual (ascospores) and asexual (conidia) spores [4]. Ascospores are produced and discharged from the perithecia during

Competing Interests: The authors have declared that no competing interests exist.

flowering and function as primary inocula [2, 5]. The initial structures or associated hyphae of the perithecia also serve as survival structures for overwintering [2, 5]. Conidia are responsible for secondary infections that are produced from sporodochia present on infected crops [5]. The biological processes of sexual and asexual sporulation in *F. graminearum* are under precise temporal and spatial regulation related to various cellular processes [6–11].

The Ccr4-Not complex is an evolutionarily conserved multi-subunit complex required for numerous cellular processes [12]. Decades of studies on model eukaryotes have revealed that the Ccr4-Not complex regulates multiple nuclear and cytoplasmic steps in gene expression, such as transcription initiation, mRNA elongation, mRNA degradation, translation, and protein degradation [12–16]. In *Saccharomyces cerevisiae*, the complex consists of nine proteins, including five ScNot proteins, three ScCaf proteins, and one ScCcr4 protein [17, 18]. The ScNot proteins (ScNot1–5) are negative regulators of genes lacking a canonical TATA box [19]. The *ScCCR4* (carbon catabolite repression) gene positively regulates glucose-repressible enzymes [20]. The ScCaf (ScCCR4 associated factor) proteins ScCaf1 (also known as ScPop2), ScCaf40, and ScCaf130 physically interact with ScCcr4 [21, 22]. Other proteins, including ScCaf4, ScCaf16, ScDhh1, and ScBtt1, have also been shown to associate with the core of the Ccr4-Not complex [14]. In human cells, two genes (*CNOT7* and *CNOT8*) are orthologous to yeast *ScCAF1*, and ScCcr4 orthologs are also encoded by separated genes, *CNOT6* and *CNOT6L* [23]. In contrast, there is only one gene (*CNOT3*) ortholog for yeast *ScNOT3* and *ScNOT5*, which likely originated from a gene duplication event in yeast.

Yeast *ScNOT5* is involved in diverse cellular processes, including maintaining cell wall integrity, carbon catabolite repression, and filamentation [14, 24], and it has recently been identified as an essential cellular regulator linking transcription, mRNA degradation, and translation [25]. *CaNOT5* is important in morphogenesis and virulence [26], and deletion of *CaNOT5* affects cell wall structure and adherence properties in *Candida albicans* [27]. In humans, *CNOT3* is an important regulator of biological processes such as retinal homeostasis, heart physiology, and stem cell self-renewal [28–30].

In a previous work, a systemic functional analysis identified transcription factors (TFs) related to various developmental processes and virulence in *F. graminearum* [9]. *FgNOT3* (FGSG_13746) was shown to encode the ScNot3 homolog, and $\Delta Fgnot3$ mutants showed pleiotropic defects in vegetative growth, sexual reproduction, secondary metabolite production, and virulence. We hypothesized that *FgNot3* is involved in diverse regulation, leading to severe impacts on numerous features of the fungus. In the present study, we report an in-depth functional analysis of *FgNot3*, a member of the Ccr4-Not complex, in *F. graminearum*. Furthermore, we demonstrate how the functions of *FgNot3* are conserved in this fungus and elucidate the involvement of the Not module in the developmental stages of *F. graminearum*.

Materials and Methods

Fungal strains and media

The *F. graminearum* wild-type strain Z-3639 [31] and the mutants used in this study are listed in Table 1. For genomic DNA (gDNA) isolation, each strain was inoculated in 5 ml of complete medium (CM) and incubated at 25°C for 3 days on a rotary shaker at 150 rpm. For fungal sporulation, the conidia of all strains were induced on yeast malt agar (YMA) [32] and in carboxymethyl cellulose (CMC) medium [33]. A rice culture was used to evaluate trichothecene and zearalenone (ZEA) production [34]. Other media used in this study were prepared and used according to the instructions in the *Fusarium* laboratory manual [4]. The wild-type and transgenic strains were stored as mycelia and conidia in 20% glycerol at -80°C.

Table 1. *F. graminearum* strains used in this study.

Strain	Genotype	Reference, source, or parent strains
Z-3639	Wild-type	[31]
hH1-GFP	<i>hH1::hH1-GFP-HYG</i>	[35]
mat1g	Δ <i>mat1-1::GEN hH1::hH1-GFP-HYG</i>	[35]
Δ <i>Fgnot3</i>	Δ <i>Fgnot3::GEN</i>	[9]
FgNot3c	Δ <i>Fgnot3::FgNOT3-HYG</i>	This study
Δ <i>Fgnot3-g</i>	Δ <i>Fgnot3::GEN hH1-GFP-HYG</i>	This study
Δ <i>Fgnot2</i>	Δ <i>Fgnot2::GEN</i>	This study
FgNot2c	Δ <i>Fgnot2::FgNOT2-HYG</i>	This study
Δ <i>Fgnot4</i>	Δ <i>Fgnot4::GEN</i>	This study
FgNot4c	Δ <i>Fgnot4::FgNOT4-HYG</i>	This study

doi:10.1371/journal.pone.0147481.t001

Nucleic acid manipulation, primers, and PCR conditions

The gDNA was extracted as previously described [4]. Restriction endonuclease digestion, agarose gel electrophoresis, gel blotting, and DNA blot hybridization were performed in accordance with standard techniques [36]. The polymerase chain reaction (PCR) primers (S1 Table) used in this study were synthesized by an oligonucleotide synthesis facility (Bionics, Seoul, Korea).

Genetic manipulations and fungal transformations

For complementation of the Δ *Fgnot3* deletion mutants, the wild-type *FgNOT3* allele from *F. graminearum* strain Z-3639 was amplified using the Not3-5F com/Not3-3N com primer pair. The hygromycin resistance cassette (*HYG*) was amplified from the pBCATPH vector using the pBCATPH/comp 5'For/pBCATPH/comp 3'Rev primer pair [37]. The resulting amplicons were fused by double-joint (DJ) PCR as previously described [38]. The final PCR constructs were obtained by nested PCR and transformed into the Δ *Fgnot3* deletion mutants as described previously [39].

To generate *FgNOT2* deletion mutants, the 5'- and 3'-flanking regions of the *FgNOT2* gene and a geneticin resistance cassette (*GEN*) were amplified from Z-3639 and pII99, respectively, and were fused by DJ PCR. The subsequent procedures for the third round of PCR and transformation were the same as for complementation using the *FgNOT3* gene of *F. graminearum*. The *FgNOT4* deletion mutants were produced using the same strategy. The same strategy used for the generation of FgNot3c strains was also applied for the complementation of the Δ *Fgnot2* and Δ *Fgnot4*.

Conidial production and morphology

After each strain was incubated in 50 ml of CM for 72 h at 25°C on a rotary shaker (150 rpm), mycelia of each strain were harvested and washed twice with distilled water. To induce conidiation, harvested mycelia were spread on YMA and incubated for 48 h at 25°C under near-UV light (wavelength: 365 nm, HKiv Import & Export Co., Ltd., Xiamen, China). Conidia were collected using distilled water, filtered through cheesecloth, washed, and resuspended in distilled water. After inoculating a 1 ml conidial suspension (1×10^6 conidia/ml) of each strain in 50 ml of CMC and incubating for 5 days at 25°C on a rotary shaker (150 rpm), the number of conidia produced was counted to measure conidial production with a hemocytometer (Superior, Marienfeld, Germany). For observation of conidial morphology, the conidia produced by each

strain on YMA were harvested, and differential interference contrast (DIC) images were obtained using a DE/Axio Imager A1 microscope (Carl Zeiss, Oberkochen, Germany).

Germination assay

To evaluate germination rates, conidial suspensions (1×10^6 conidia/ml) of each strain were inoculated into 20 ml of CM and MM and incubated at 25°C on a rotary shaker (150 rpm). The germinated conidia per 100 total conidia were counted at 0, 4, 6, 8, 10, 12, 24, 36, 48, and 60 h after inoculation. Conidial germination was defined as the point at which the length of the germ tube is the same as the width of the conidium. The experiments were performed twice with three replicates for each time point.

Outcrosses and virulence test

For self-fertilization, mycelia grown on carrot agar for 5 days were mock-fertilized with a 2.5% Tween 60 solution to induce sexual reproduction as previously described [4]. For outcrosses, mycelia of the female strain grown on carrot agar plates were fertilized with 1 ml of male strain conidia (1×10^6 conidia/ml). The heterothallic mat1g (Δ mat1-1::GEN hH1::hH1-GFP-HYG) strain [35] was used as a tester strain for outcrosses. After sexual induction, the fertilized cultures were incubated for 7 days under near-UV light (HKiv Import & Export Co., Ltd.) at 25°C.

A virulence test of the fungal strains was performed using the wheat cultivar Eunpamil as previously described [40]. Briefly, 10 μ l of conidial suspensions (1×10^6 conidia/ml) obtained from each strain was point-inoculated into a spikelet of the wheat head at early anthesis. Infected plants were incubated in a humidity chamber for 3 days and subsequently transferred to a green house. After 21 days, the number of spikelets showing disease symptoms was counted.

Quantification of mycotoxins and fungal ergosterol

For trichothecene analysis, the 3-week-old rice cultures were ground and extracted with an ethyl acetate/methanol mixture (4:1, v/v) as previously described [34]. The extracts were purified using MycoSep[®] 225 Trich Multifunctional columns (Romer Labs, Inc., Union, MO, USA) and then concentrated to dryness. A portion of each extract was derivatized with Sylon BZT (BSA + TMCS + TMSI, 3:2:3, Supelco, Bellefonte, PA, USA) and analyzed using a Shimadzu QP-5000 gas chromatograph-mass spectrometer (GC-MS; Shimadzu, Kyoto, Japan). ZEA was extracted from rice cultures using the same strategy and analyzed using a HPLC system with a RF-10A XL fluorescence detector (Shimadzu) [34]. To quantify fungal ergosterol, ground rice cultures (1 g) were extracted in 4 ml of chloroform/methanol (2:1, v/v) as previously described [41]. Ergosterol was analyzed using a HPLC system with a 4.6 U ODS column (250×4.6 mm, Phenomenex, Madrid Avenue Torrance, CA, USA) and an UV detector (Shimadzu) set to measure absorbance at 282 nm. Quantities were determined by comparing peak areas of samples to those of a standard curve generated from HPLC-grade ergosterol (Sigma-Aldrich, St. Louis, Missouri, USA). The experiments were repeated three times.

Quantitative real-time (qRT)-PCR

The total RNA of the wild-type and Δ *Fgnot3* strains was extracted from mycelia at 18 h after inoculation in CMC using an Easy-Spin Total RNA Extraction kit (Intron Biotech, Seongnam, Korea) [42]. First-strand cDNA was synthesized with the SuperScript III First-Strand Synthesis System (Invitrogen, Carlsbad, CA, USA) using oligo(dT)₂₀ according to the manufacturer's

recommendations. qRT-PCR was performed using iQ SYBR Green Master Mix (Bio-Rad, Hercules, CA, USA) and a 7500 real-time PCR system (Applied Biosystems, Foster City, CA, USA). The endogenous housekeeping gene, ubiquitin C-terminal hydrolase (*UBH*; FGSG_01231), was used for normalization [22]. The PCR assays were repeated three times with two biological replicates. The threshold cycle (ΔC_T) value of gene expression was subtracted from the ΔC_T value of each sample to obtain a $\Delta\Delta C_T$ value. The transcript level relative to the calibrator was expressed as $2^{-\Delta\Delta C_T}$ [43].

Yeast strains and complementation assay

The *S. cerevisiae* strains, BY4741 (wild-type) and YPR072w ($\Delta Scnot5$), were obtained from EUROSCARF (<http://web.uni-frankfurt.de/fb15/mikro/euroscarf/>) and maintained on yeast extract peptone dextrose (YPD) medium. The *FgNOT3* ORF was amplified from first-strand cDNA of the *F. graminearum* wild-type strain, Z-3639, with the Not3-cloning-F/Not3-cloning-R primer pair (S1 Table) by PCR, digested by BstXI and XbaI restriction enzymes, and subsequently cloned into the BstXI and XbaI sites of pYES2 (Invitrogen). The pYES2-*FgNOT3* construct was introduced into the $\Delta Scnot5$ strain using the lithium acetate method [44] after verification of the construct by sequencing (Macrogen Inc., Seoul, Korea). In addition, the pYES2 empty vector was simultaneously introduced into yeast wild-type BY4741 and $\Delta Scnot5$. Synthetic complete medium lacking uracil (SC-Ura) and supplemented with ampicillin (0.2 mg/ml) was used for the selection and isolation of transformants [44]. For the complementation assay, yeast cells were cultured for 3 days at 30°C on a rotary shaker (200 rpm) in SC-Ura supplemented with ampicillin, and the cells were then harvested and diluted in distilled water. Aliquots of 10 μ l were point-inoculated on SC-Ura supplemented with ampicillin followed by incubation for 4 days at 30°C.

Results

Molecular characterization of the *FgNOT3* gene

The Ccr4-Not complex of *S. cerevisiae* consists of two major modules, the catalytic module (ScCaf1 and ScCcr4) and the Not module (ScNot1, ScNot2, ScNot3, ScNot4, and ScNot5), and an additional two subunits, namely ScCaf40 and ScCaf130 [17, 18]. The occurrence of the subunit genes in the Ccr4-Not complex in representative species based on the STRING database [45] showed that most of these genes are highly conserved in eukaryotes (Fig 1A). However, Caf130 homologs are specifically conserved in members of the Saccharomycetaceae, such as *S. cerevisiae* and *Candida glabrata*.

Except for fungal species of the Saccharomycetaceae, only single gene-encoding proteins similar to ScNot3 or ScNot5 have been identified in other eukaryotic genomes (Fig 1A). Although Not3/5 of oomycetes, *Phytophthora infestans* and *Pythium ultimum* showed higher sequence identity with ScNot5 than ScNot3, the rest of the single proteins were homologs for ScNot3. Previous reports have also shown that Not5 is not conserved in animals and is specific for the Saccharomycetaceae [46]. Phylogenetic analyses of Not3 homologs showed that Not3 homologs in filamentous fungi were clustered into a separate group relative to yeasts and animals (Fig 1B).

BLASTp searches for both ScNot3 and ScNot5 in the *F. graminearum* genome (<http://www.broadinstitute.org>) identified the FGSG_13746 locus encoding 582 amino acids (30% and 27% overall identity to ScNot3 and ScNot5, respectively). The protein harbored two significant domains (IPR007207 and IPR007282) similar to those of both ScNot3 and ScNot5 (Fig 1C). Further analysis of the conserved protein sequences of partial N-terminal regions showed that FGSG_13746 shares 55% and 50% identity with those of ScNot3 and ScNot5, respectively. The

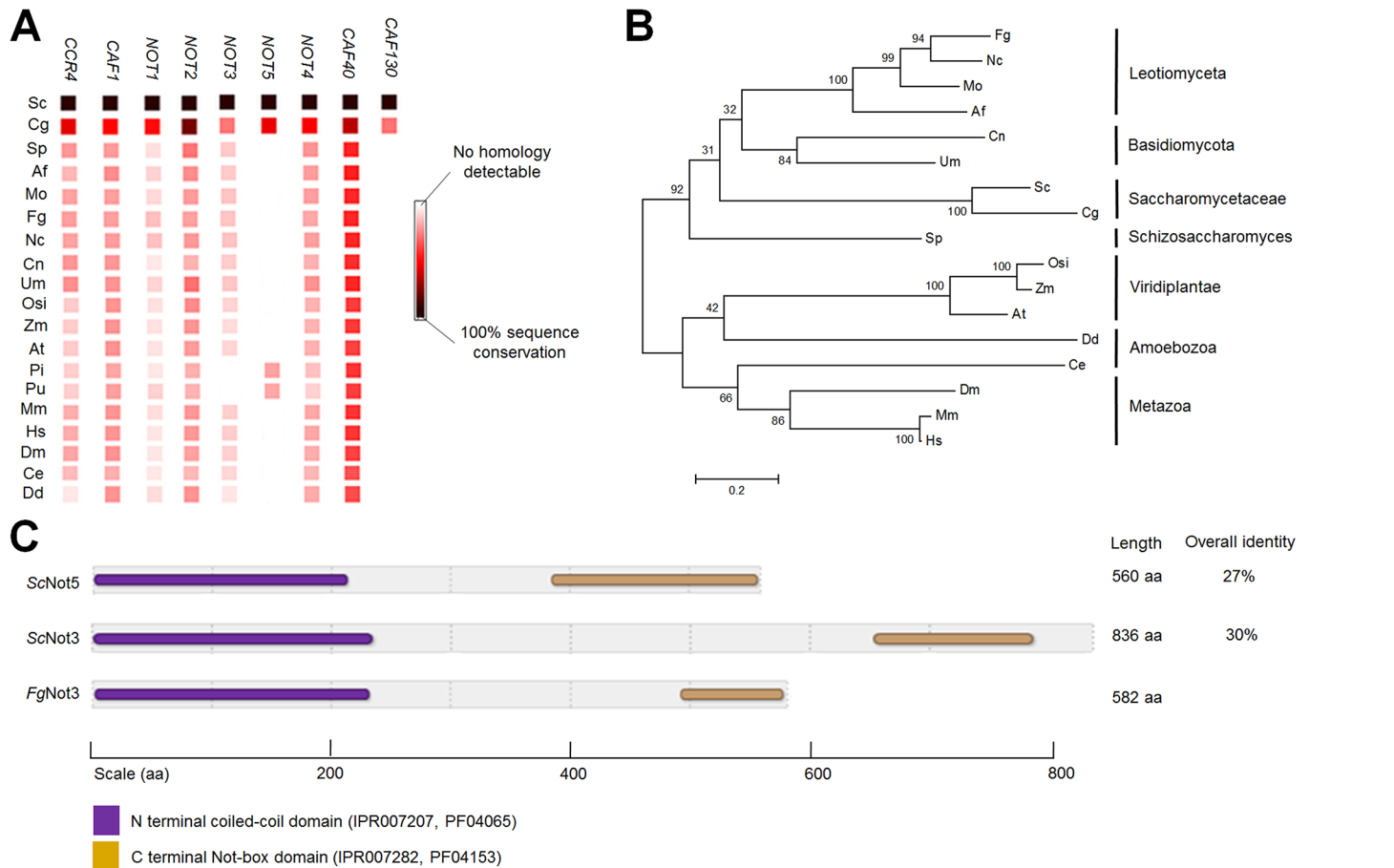


Fig 1. Molecular characterization of *FgNot3*. (A) Occurrences of subunit genes of the Ccr4-Not complex homologs in representative species. The image was constructed using the STRING database [45]. Sc, *Saccharomyces cerevisiae*; Cg, *Candida glabrata*; Sp, *Schizosaccharomyces pombe*; Af, *Aspergillus fumigatus*; Mo, *Magnaporthe oryzae*; Fg, *Fusarium graminearum*; Nc, *Neurospora crassa*; Cn, *Cryptococcus neoformans*; Um, *Ustilago maydis*; Osi, *Oryza sativa Indica*; Zm, *Zea mays*; At, *Arabidopsis thaliana*; Pi, *Phytophthora infestans*; Pu, *Pythium ultimum*; Mm, *Mus musculus*; Hs, *Homo sapiens*; Dm, *Drosophila melanogaster*; Ce, *Caenorhabditis elegans*; Dd, *Dictyostelium discoideum*. (B) Phylogenetic tree of homologs of the Not3 subunit from the Ccr4-Not complex from representative species constructed using amino acid sequence comparison. (C) Schematic presentation of the conserved regions of Not3 subunit homologs between *S. cerevisiae* and *F. graminearum*. The percentage of identity between two proteins was calculated using the ALIGN algorithm (global alignment with no short-cuts). Different shadings denote the domain entries in the InterPro database (<http://www.ebi.ac.uk/interpro/>) and the HMMPham database (<http://pfam.sanger.ac.uk/>).

doi:10.1371/journal.pone.0147481.g001

human C-terminal region of Not3 also shows 24% overall identity to both ScNot3 and ScNot5 although their N-terminal regions share 41% and 39% identity with those of ScNot3 and ScNot5, respectively [47]. Based on these combined results, we designated the protein encoded by FGSG_13746 as *FgNot3*.

Effects of *FgNOT3* deletion on vegetative growth, conidiogenesis, and germination

The *FgNOT3* deletion mutants were obtained from a mutant library of *F. graminearum* TF deletions [9]. For genetic complementation, the construct containing the *FgNOT3* open reading frame (ORF) fused with *HYG* was introduced into the protoplast of the $\Delta Fgnot3$ strain (S1 Fig). Southern blot analysis showed that the construct successfully replaced *GEN* in the genome of the complementation strain, resulting in *FgNot3c* strains. The $\Delta Fgnot3$ strains showed

markedly reduced radial growth (~50%) and aerial mycelia on both complete medium (CM) and minimal medium (MM) (Fig 2A).

To further determine the features affecting the defective growth of the $\Delta Fgnot3$ mutants, we performed microscopic observation. Deletion of *FgNOT3* resulted in a hyper-branching phenotype compared to the wild-type strain (Fig 2B). Furthermore, the hyphae of $\Delta Fgnot3$ mutants tended to be abnormally swollen, and the swollen hyphae resulted in distorted branching (Fig 2C). These results demonstrated that *FgNOT3* is required for normal growth and mycelial morphology in *F. graminearum*.

Deletion of *FgNOT3* also resulted in severe defects in asexual sporulation. The conidial production of the $\Delta Fgnot3$ strain in CMC medium was significantly reduced compared to the wild-type and complemented strains (Fig 3A). Moreover, conidia of $\Delta Fgnot3$ strains were abnormally shaped (Fig 3B). The conidia of the $\Delta Fgnot3$ strains were shorter and wider than the wild-type (Table 2 and Fig 3B). Deletion of *FgNOT3* also resulted in a reduced septum number.

To determine how deletion of *FgNOT3* affects conidiogenesis in *F. graminearum*, we generated $\Delta Fgnot3$ -g strains ($\Delta Fgnot3::GEN\ hH1$ -GFP-HYG) by an outcross between the mat1g [35] and $\Delta Fgnot3$ strains. Dozens of ascospores were isolated, and their genotypes were confirmed by fluorescence microscopy and PCR. The hH1-GFP strain carrying the wild-type allele of *FgNOT3* initially produced phialides from the hyphae, and mature phialide cells continuously produced conidia (Fig 3C). Additionally, conidia were often directly produced from the hyphae. In contrast, deletion of the *FgNOT3* mostly abolished phialide production, and most conidia were directly produced from the hyphae (Fig 3C). All of these defects were restored to wild-type levels in the *FgNot3c* complemented strains.

To test the hypothesis that *FgNot3* plays a role in regulating the expression of genes related to conidiogenesis, we compared the transcript levels of representative conidiation-related genes in the wild-type and $\Delta Fgnot3$ deletion mutant strains [6–9]. Transcript levels of four genes, namely *STUA*, *HTF1*, *REN1*, and *FLBC*, were significantly decreased in the $\Delta Fgnot3$

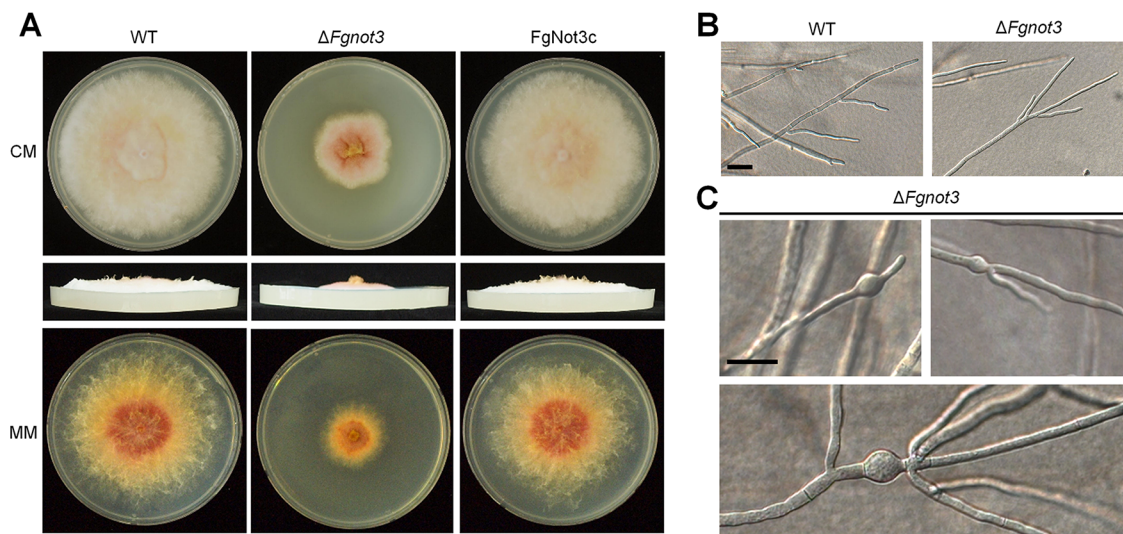


Fig 2. The vegetative growth of $\Delta Fgnot3$ mutants. (A) Mycelial growth on complete medium (CM) and minimal medium (MM). The pictures were taken 5 days after inoculation. The pictures were taken from the upper (top) and the side (middle) of the plates. (B) Microscopic observation of hyphae. The differential interference contrast (DIC) images were taken 2 days after inoculation. Scale bar = 50 μ m. (C) Swollen hyphae of $\Delta Fgnot3$ mutants on CM agar. Scale bar = 50 μ m. WT, *F. graminearum* wild-type strain Z-3639; $\Delta Fgnot3$, *FgNOT3* deletion mutant; FgNot3c, $\Delta Fgnot3$ -derived strain complemented with *FgNOT3*.

doi:10.1371/journal.pone.0147481.g002

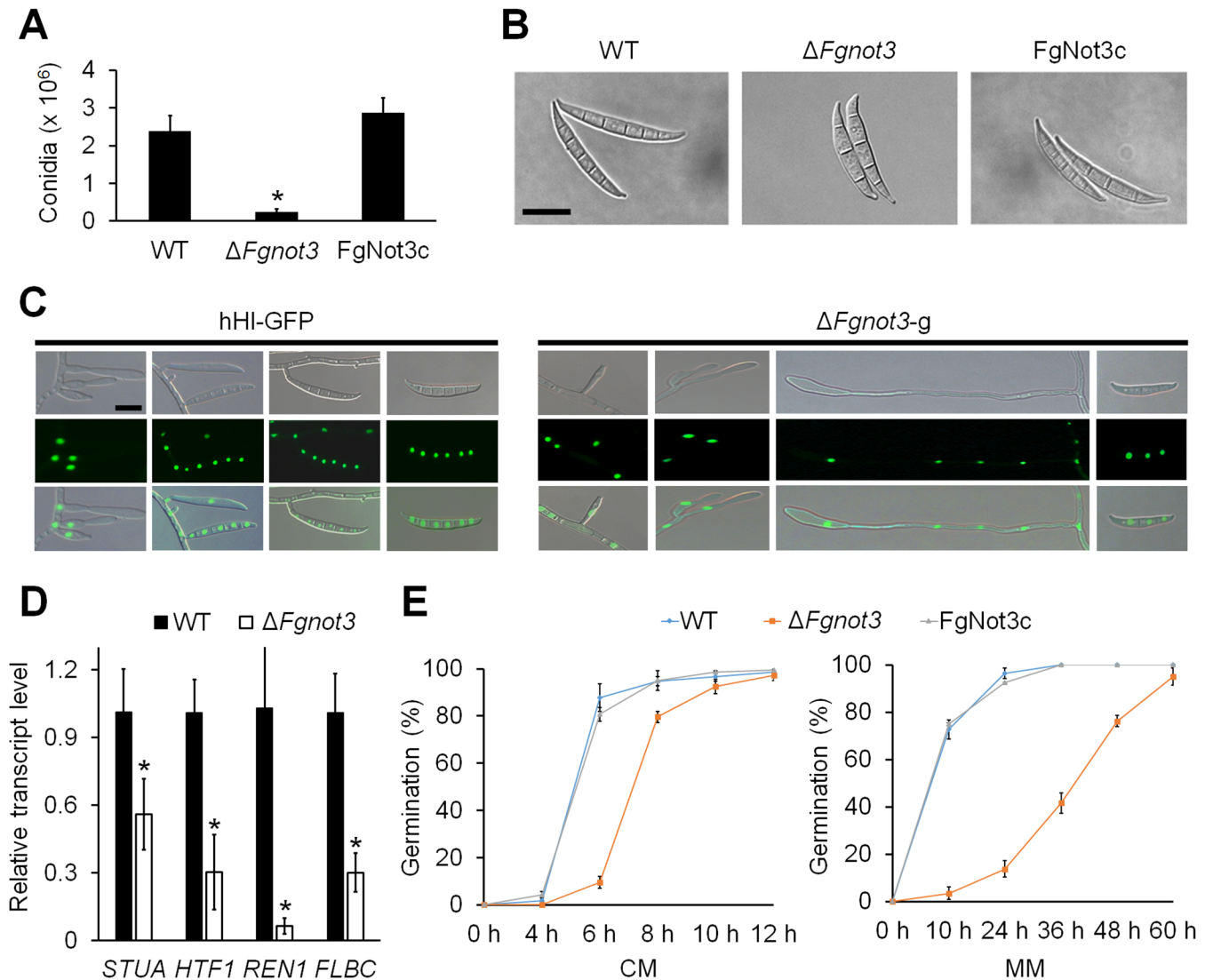


Fig 3. Conidiation and germination of $\Delta Fgnot3$ mutants. (A) Conidial production. The number of conidia was counted after 5 days of incubation in CMC. The values were generated based on three biological replicates. Significant differences ($P < 0.05$) are indicated with an asterisk. (B) Conidial morphology. Conidia were induced on YMA and subsequently observed by DIC. Scale bar = 20 μ m. (C) Morphology of conidiophores in *F. graminearum* strains. Pictures were taken 1 to 3 days after conidium induction. Scale bar = 10 μ m. (D) Relative transcript levels of genes related to conidiation. Total RNA of the wild-type and $\Delta Fgnot3$ strains was extracted 18 h after inoculation in CMC. The relative transcript levels of each subunit gene in the wild-type were arbitrarily set to 1. Significant differences ($P < 0.05$) are indicated with an asterisk. (E) Germination rate. The percentage of conidium germination in CM and MM. WT, *F. graminearum* wild-type strain Z-3639; $\Delta Fgnot3$, *FgNOT3* deletion mutant; FgNot3c, $\Delta Fgnot3$ -derived strain complemented with *FgNOT3*.

doi:10.1371/journal.pone.0147481.g003

mutants compared to wild-type (Fig 3D). Interestingly, transcript levels of *ABAA* and *WETA*, the transcription factors specifically involved in conidiogenesis in *F. graminearum* [10, 11], were not altered when *FgNOT3* was deleted (data not shown).

The conidia germination rates of $\Delta Fgnot3$ mutants were greatly reduced in both CM and MM compared to wild-type (Fig 3E). Approximately 90% of conidia in the wild-type strain germinated 6 h after inoculation in CM, whereas only approximately 10% of conidia germinated in the $\Delta Fgnot3$ mutants (Fig 3E). Furthermore, only approximately 16% of $\Delta Fgnot3$ mutant conidia germinated in MM 24 h after inoculation, whereas most wild-type conidia were germinated after 24 h. Although the germinated hyphae of all strains showed an identical morphology

Table 2. Conidial morphology and virulence of $\Delta Fgnot3$ mutants.

Strain	Conidial morphology ^a			Virulence (disease index) ^c
	Length (μm)	Width (μm)	No. of septa	
Z-3639	46.8 \pm 1.8A ^b	6.1 \pm 0.1A	4.0 \pm 0.1A	9.7 \pm 4.1A
$\Delta Fgnot3$	41.2 \pm 0.2B	7.1 \pm 0.4B	3.4 \pm 0.1B	0.45 \pm 0.3B
FgNot3c	45.3 \pm 1.3A	6.2 \pm 0.1A	4.0 \pm 0.1A	9.6 \pm 2.6A

^a Conidia were harvested from a 1-day-old YMA culture.

^b The presented data are average values \pm standard deviations. Values within a column with different letters are significantly different ($P < 0.05$) based on Tukey's HSD test.

^c The disease index (number of diseased spikelets per wheat head) of the strains was measured 21 days after inoculation.

doi:10.1371/journal.pone.0147481.t002

up to 24 h after inoculation in CM (S2 Fig), the germinated hyphae of $\Delta Fgnot3$ mutants exhibited swollen tips 26 h after inoculation (S2 Fig and Fig 2C). All defects of the $\Delta Fgnot3$ mutants were restored in the FgNot3c complemented strains.

FgNOT3 is important for sexual development and virulence

The fertility of the *F. graminearum* strains was determined on carrot agar. In self-fertility, the wild-type strains began to produce detectable perithecial initials 3 days after sexual induction, and mature perithecia were produced after an additional 3 or 4 days of incubation (Fig 4A). In contrast to wild-type, the $\Delta Fgnot3$ mutants only produced a few perithecium initials that did not mature.

Subsequently, we determined the female and male fertilities of the $\Delta Fgnot3$ mutants based on outcross analyses. When the $\Delta Fgnot3$ mutant was spermatized with wild-type or $\Delta mat1$ strains, no mature perithecium was produced, similar to the self-cross of the $\Delta Fgnot3$ mutants (Fig 4A). However, when the $\Delta Fgnot3$ mutant was used as a male in the outcross of $\Delta mat1$ (female) \times $\Delta Fgnot3$ (male), normal perithecia were produced, and the progeny with or without the hH1-Gfp signal were segregated 1:1 in accordance with Mendelian genetics, suggesting that *FgNOT3* is not necessary for male fertility (Fig 4B). The sexual defects of the $\Delta Fgnot3$ mutants were recovered in the FgNot3c strains.

To evaluate the pathogenicity of the $\Delta Fgnot3$ mutants in flowering wheat heads, conidial suspensions of each strain were point-inoculated on spikelets. The results showed that wild-type and FgNot3c strains caused typical head blight symptoms 21 days after inoculation, whereas the $\Delta Fgnot3$ strains were unable to spread from the inoculated spikelet to adjacent spikelets on the heads (Table 2 and Fig 4C).

FgNOT3 is required for normal growth under high-temperature conditions

To characterize the roles of *FgNOT3* in environmental stress responses, we examined the sensitivity of the $\Delta Fgnot3$ mutants to various stresses, including carbon and nitrogen starvation, osmotic and oxidative stresses, cell wall-damaging agents, fungicide exposure, and thermal stresses. There were no specific stresses or agents that affected the growth of $\Delta Fgnot3$ mutants as previously described (data not shown). However, we identified the role of *FgNOT3* in adaptation to thermal stress in *F. graminearum*. The $\Delta Fgnot3$ mutants exhibited increased sensitivity to high temperature and could not grow at 31°C (Fig 5).

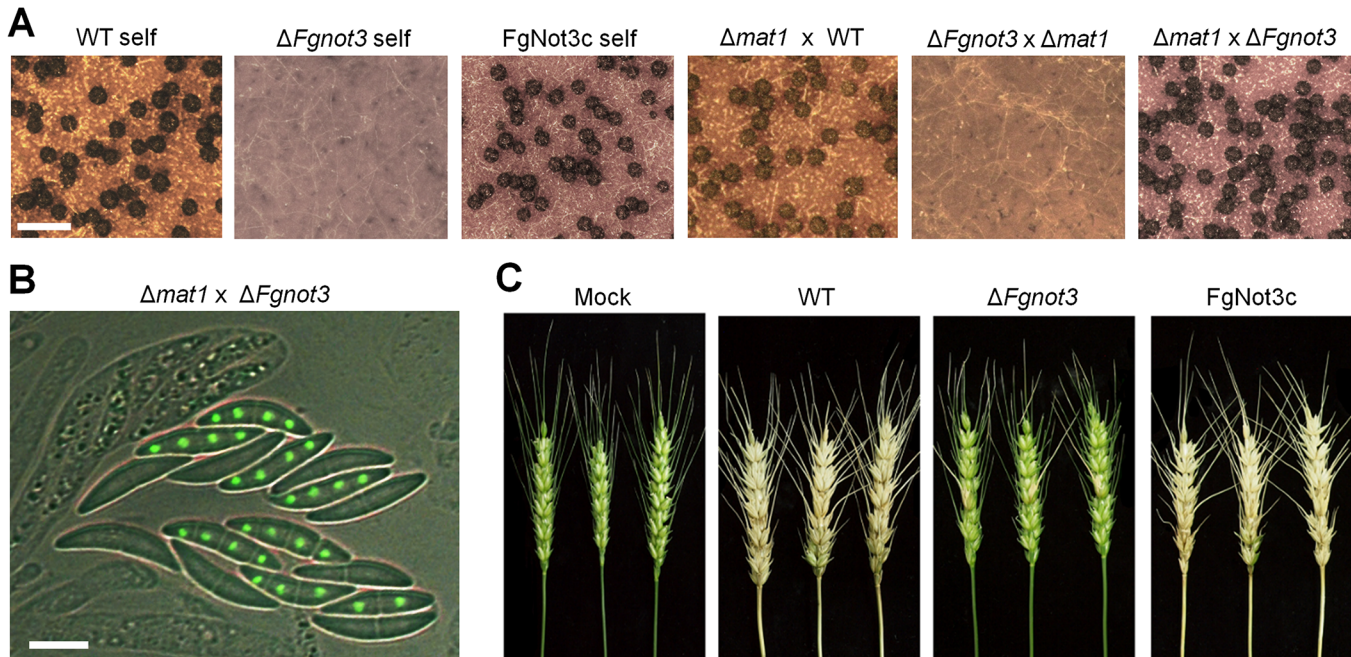


Fig 4. The sexual development and virulence of $\Delta Fgnot3$ mutants. (A) Fertility tests. Each strain was inoculated on carrot agar and mock-fertilized (self-cross) or outcrossed with the corresponding male strains (WT, $\Delta Fgnot3$ and $\Delta mat1$). The photographs were taken 7 days after sexual induction. Scale bar = 500 μm . (B) Asci of an outcross $\Delta mat1 \times \Delta Fgnot3$. Eight ascospores of an ascus from the $\Delta mat1 \times \Delta Fgnot3$ outcross showing 1:1 segregation with and without Gfp-tagged histone H1. The photographs were taken 9 days after sexual induction. Scale bar = 10 μm . (C) Virulence on wheat heads. The center spikelet of each wheat head was injected with 10 μl of a conidial suspension. Pictures were taken 21 days after inoculation. Mock, negative control mock-inoculated with 0.01% of Tween 20; WT, *F. graminearum* wild-type strain Z-3639; $\Delta Fgnot3$, *FgNOT3* deletion mutant; FgNot3c, $\Delta Fgnot3$ -derived strain complemented with *FgNOT3*.

doi:10.1371/journal.pone.0147481.g004

FgNot3 functions together with other Not subunits of the Ccr4-Not complex

The effects of *FgNOT3* deletion on the transcript levels of nine putative Ccr4-Not complex subunit genes were analyzed during conidiation (Fig 6). Five genes (homologs for *CCR4*, *CAF1*, *CAF40*, *CAF130*, and *DDH1*) showed similar transcript levels between the wild-type and $\Delta Fgnot3$ strains. However, the transcript levels of *FgNOT1* and *FgNOT4* in the $\Delta Fgnot3$ mutants were significantly decreased compared with the wild type (Fig 6). The *FgNOT2* transcript levels of the $\Delta Fgnot3$ mutants were greatly increased, showing more than 6-fold higher expression than wild type (Fig 6).

Because *FgNOT1* is an essential gene [9] and $\Delta Fgnot3$ showed pleiotropic defects, we sought to determine how other Not subunits affect the developmental stages of *F. graminearum*. To characterize their biological functions, we generated deletion and complementation mutants of *FgNOT2* (FGSG_12685) and *FgNOT4* (FGSG_09233) via homologous recombination (S4 Fig). We found that the radial growth, conidial production, conidial morphology, sexual development, and virulence of both $\Delta Fgnot2$ and $\Delta Fgnot4$ mutants were severely impaired compared to wild type, similar to the observed phenotypes of the $\Delta Fgnot3$ strains (Figs 7 and 8 and Table 3). In particular, deletion of *FgNOT2* and *FgNOT4* resulted in markedly reduced radial growth compared to the wild-type and complemented strains (Fig 7). Furthermore, $\Delta Fgnot2$ and $\Delta Fgnot4$ mutants also exhibited increased sensitivity to high temperature (Fig 5).

Conidial production of both the $\Delta Fgnot2$ and $\Delta Fgnot4$ mutants was similarly reduced compared to wild type (Table 3). Deletion of *FgNOT2* resulted in more severe defects in conidial

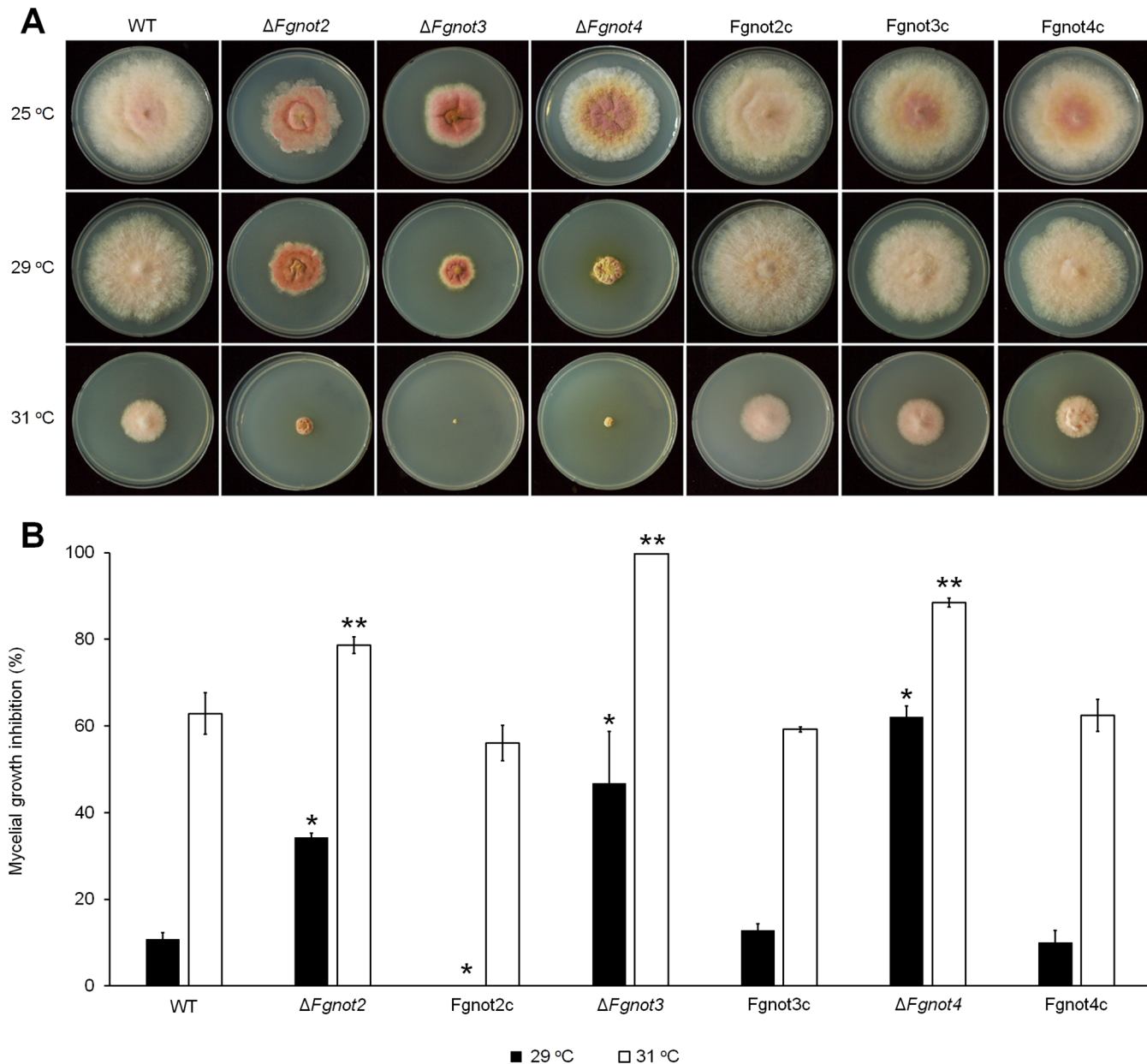


Fig 5. Sensitivity to thermal stress. (A) Mycelial growth at different temperatures. (B) Mycelial growth inhibition rate. Each strain was inoculated on CM and incubated at 25°C, 29°C, and 31°C for 5 days. The percentage of the mycelial radial growth inhibition was calculated using the following equation: $[(C-N)/C] \times 100$, where C is colony diameter of the control (at 25°C), and N is that of treatments (at 29°C and 31°C) as previously described [48]. The values were generated based on three biological replicates. The significance of differences between the wild-type and each strain was calculated using Student's t-test. Significant differences ($P < 0.05$) are indicated with an asterisk for the 29°C condition or a double asterisk for the 31°C condition. WT, *F. graminearum* wild-type strain Z-3639; $\Delta Fgnot2$, *FgNOT2* deletion mutant; $\Delta Fgnot3$, *FgNOT3* deletion mutant; $\Delta Fgnot4$, *FgNOT4* deletion mutant; FgNot2c, $\Delta Fgnot2$ -derived strain complemented with *FgNOT2*; FgNot3c, $\Delta Fgnot3$ -derived strain complemented with *FgNOT3*; FgNot4c, $\Delta Fgnot4$ -derived strain complemented with *FgNOT4*.

doi:10.1371/journal.pone.0147481.g005

morphologies than *FgNOT4* deletion (Table 3 and Fig 8A). Whereas the $\Delta Fgnot3$ mutants showed an almost complete lack of phialide formation, the $\Delta Fgnot2$ and $\Delta Fgnot4$ mutants mainly produced normal phialides and conidia (Fig 8B). Approximately 30% of the phialides of both $\Delta Fgnot2$ and $\Delta Fgnot4$ mutants were produced as cluster forms with abnormal shapes.

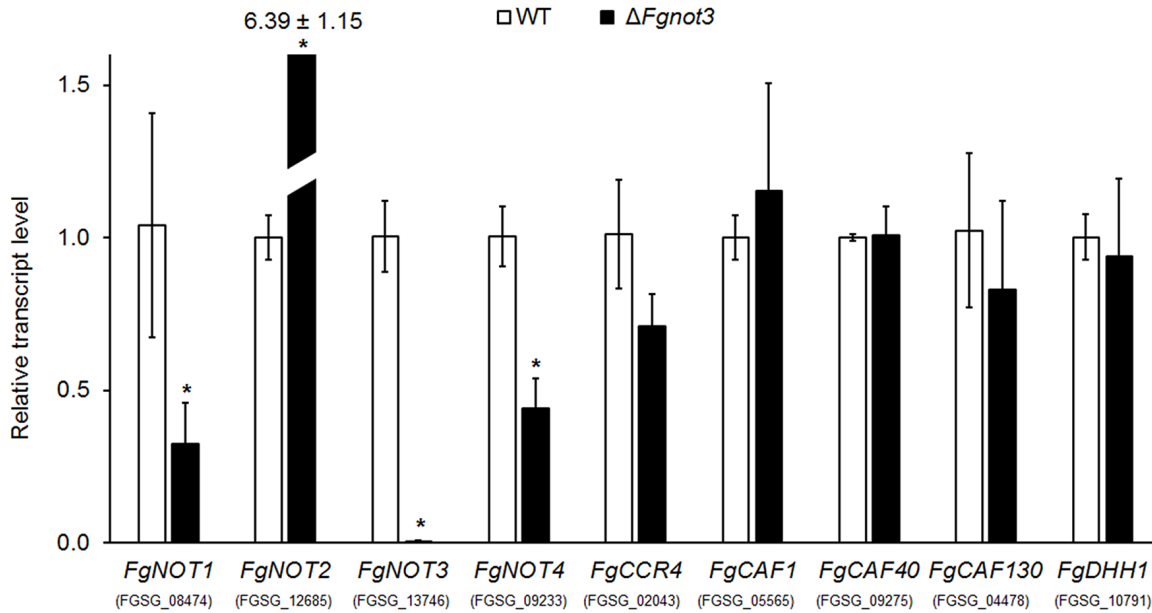


Fig 6. Relative transcript levels of subunits of the Ccr4-Not complex during the conidium induction stage. Total RNA of the wild-type and $\Delta Fgnot3$ strains was extracted 18 h after inoculation in CMC. The relative transcript levels of each subunit in the Ccr4-Not complex in wild type were arbitrarily set to 1. Significant differences ($P < 0.05$) are indicated with an asterisk.

doi:10.1371/journal.pone.0147481.g006

We found that deletion of *FgNOT2* and *FgNOT4* also resulted in a loss of self and female fertilities (Fig 8C and 8D) and a significant decrease in virulence on wheat heads (Table 3 and Fig 8E). All of these defects of the $\Delta Fgnot2$ and $\Delta Fgnot4$ mutants were restored to wild type levels in the corresponding complemented strains.

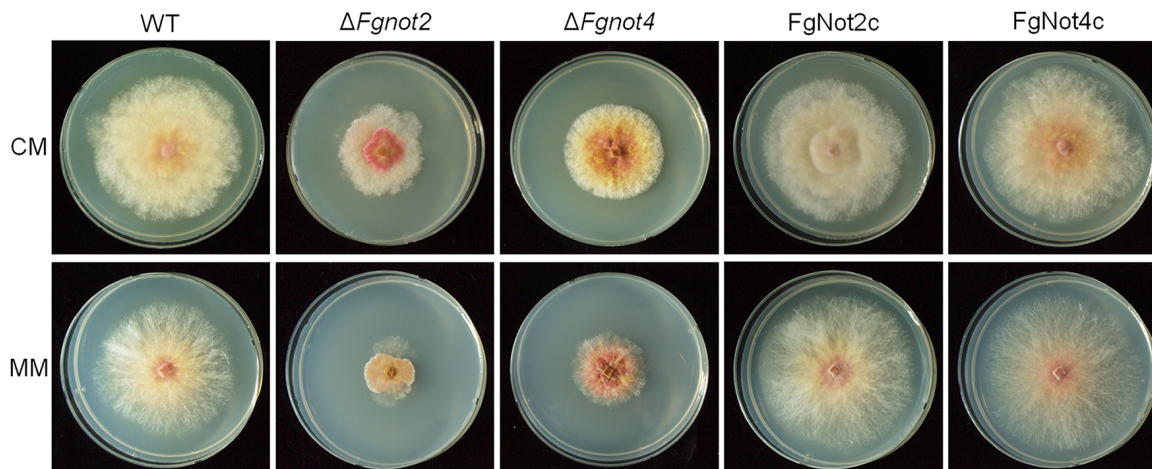


Fig 7. The vegetative growth of $\Delta Fgnot2$ and $\Delta Fgnot4$ mutants. Pictures were taken 4 days after inoculation on CM and MM. WT, wild-type strain Z-3639; $\Delta Fgnot2$, *FgNOT2* deletion mutant; *FgNot2c*, $\Delta Fgnot2$ -derived strain complemented with *FgNOT2*; $\Delta Fgnot4$, *FgNOT4* deletion mutant; *FgNot4c*, $\Delta Fgnot4$ -derived strain complemented with *FgNOT4*.

doi:10.1371/journal.pone.0147481.g007

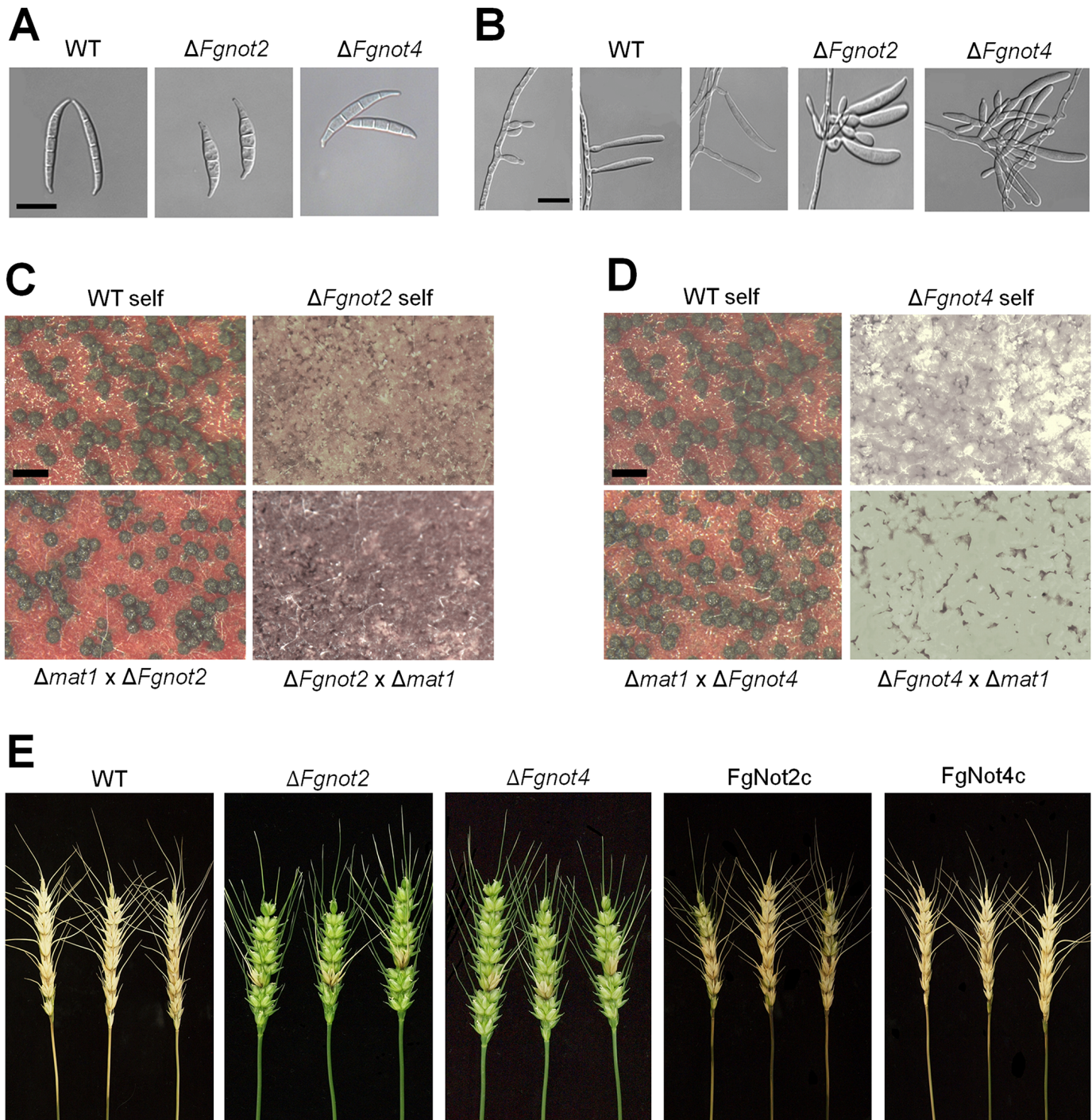


Fig 8. Phenotypes of $\Delta Fgnot2$ and $\Delta Fgnot4$ mutants. (A) Conidial morphology. Conidia were induced on YMA and subsequently observed by DIC. Scale bar = 20 μ m. (B) Morphologies of conidiophores. Scale bar = 20 μ m. (C-D) Fertility tests of $\Delta Fgnot2$ (C) and $\Delta Fgnot4$ (D). Each strain was inoculated on carrot agar and mock fertilized (self-cross) or outcrossed with a respective male strain (WT, $\Delta Fgnot2$, $\Delta Fgnot4$, and $\Delta mat1$). Pictures were taken 7 days after sexual induction. Scale bar = 500 μ m. (E) Virulence on wheat heads. The center spikelet of each wheat head was injected with 10 μ l of a conidial suspension. Pictures were taken 21 days after inoculation. WT, wild-type strain Z-3639; $\Delta Fgnot2$, $FgNOT2$ deletion mutant; $FgNot2c$, $\Delta Fgnot2$ -derived strain complemented with $FgNOT2$; $\Delta Fgnot4$, $FgNOT4$ deletion mutant; $FgNot4c$, $\Delta Fgnot4$ -derived strain complemented with $FgNOT4$.

doi:10.1371/journal.pone.0147481.g008

Table 3. Vegetative growth, conidial production, conidial morphology, and virulence of $\Delta Fgnot2$ and $\Delta Fgnot4$ mutants.

Strain	Radial growth (mm) ^a	Conidial production(10 ⁶ /ml) ^b	Conidial morphology ^c			Virulence (disease index) ^d
			Length (μ m)	Width (μ m)	No. of septa	
Z-3639	64.4 \pm 1.1A ^e	3.1 \pm 0.5A	45.5 \pm 0.9A	5.8 \pm 0.2A	4.0 \pm 0.1A	9.8 \pm 2.3A
$\Delta Fgnot2$	50.2 \pm 1.2B	2.0 \pm 0.2B	42.9 \pm 0.2B	7.2 \pm 0.2B	3.3 \pm 0.1B	0.8 \pm 0.3B
FgNot2c	65.2 \pm 1.0A	2.9 \pm 0.2A	43.6 \pm 0.4B	6.1 \pm 0.1AC	4.0 \pm 0.1A	8.6 \pm 4.6A
$\Delta Fgnot4$	45.0 \pm 1.1C	2.2 \pm 0.3B	43.2 \pm 0.4B	5.9 \pm 0.1A	4.0 \pm 0.1A	2.8 \pm 2.1B
FgNot4c	65.6 \pm 1.6A	3.2 \pm 0.3A	46.4 \pm 1.0C	6.3 \pm 0.2C	4.2 \pm 0.2A	9.0 \pm 4.4A

^a Radial growth was measured 4 days after inoculation on CM plates.

^b Conidia were counted 5 days after inoculation in CMC.

^c Conidia were harvested from a 1-day-old YMA culture.

^d The disease index (number of diseased spikelets per wheat head) of the strains was measured 21 days after inoculation.

^e The presented data are average values \pm standard deviations. Values within a column with different letters are significantly different ($P < 0.05$) based on Tukey's HSD test.

doi:10.1371/journal.pone.0147481.t003

FgNOT2, *FgNOT3*, and *FgNOT4* are all involved in secondary metabolite production

Whereas $\Delta Fgnot4$ mutants only produced significantly higher levels of ZEA than the wild-type strain, deletion of both *FgNOT2* and *FgNOT3* resulted in much higher production of both trichothecenes and ZEA in rice cultures (Fig 9). These observed defects in the $\Delta Fgnot2$, $\Delta Fgnot3$, and $\Delta Fgnot4$ mutants were restored in the corresponding complemented strains.

Discussion

In this study, *FgNOT3* was found to be involved in numerous developmental stages in *F. graminearum*, including vegetative growth, asexual reproduction, sexual reproduction, secondary metabolite production, and virulence. Moreover, we provided genetic evidence that other Not subunits also have conserved roles in this fungus. Taken together, these results demonstrated

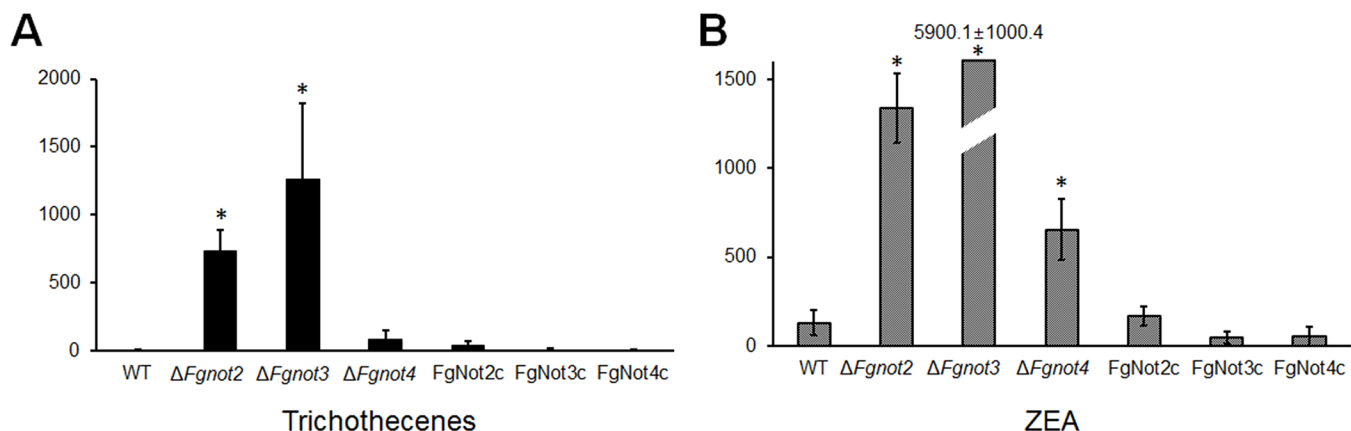


Fig 9. Mycotoxin production of $\Delta Fgnot2$, $\Delta Fgnot3$, and $\Delta Fgnot4$ mutants. Total trichothecene production or zearalenone (ZEA) production was normalized to fungal ergosterol levels with the following equation as previously described [41]: [trichothecene or ZEA production (μ g/g) / ergosterol contents (μ g/g)] \times 100. The values were generated based on three biological replicates. The significance of differences between the wild-type and each strain was calculated using Student's t-test. Significant differences ($P < 0.05$) are indicated with an asterisk. WT, wild-type strain Z-3639; $\Delta Fgnot2$, *FgNOT2* deletion mutant; FgNot2c, $\Delta Fgnot2$ -derived strain complemented with *FgNOT2*; $\Delta Fgnot3$, *FgNOT3* deletion mutant; FgNot3c, $\Delta Fgnot3$ -derived strain complemented with *FgNOT3*; $\Delta Fgnot4$, *FgNOT4* deletion mutant; FgNot4c, $\Delta Fgnot4$ -derived strain complemented with *FgNOT4*.

doi:10.1371/journal.pone.0147481.g009

that the Not module of the Ccr4-Not complex plays critical roles in the regulation of multiple and complex cellular processes and differentiation in *F. graminearum*.

FgNot3 contributes to hyphal morphogenesis and virulence in *F. graminearum*. Deletion of *FgNOT3* led to a significant reduction in mycelial production and abnormal shaped hyphae in *F. graminearum*, phenotypes similar to other model eukaryotes. Yeast ScNOT5 is involved in diverse processes, including cell wall integrity and filamentation [14, 24]. Deletion of *CaNOT5* also results in defective morphogenesis and virulence in *Candida albicans* [26]. Although the $\Delta Fgnot3$ mutants produced a considerable amount of trichothecenes, which are virulence factors [49], virulence of the mutants was completely abolished, and fungal growth was restricted to infection sites. We believe that the $\Delta Fgnot3$ mutant hyphae could not differentiate into structures required for host infection due to the attenuated morphogenesis and cellular differentiation. It has been reported that *F. graminearum* hyphae develop mats and appressoria-like structures to penetrate the host cell wall [50, 51].

FgNot3 also regulates hyphal differentiation required for both sexual and asexual reproduction in *F. graminearum*. Both ascospores and conidia are produced from highly differentiated hyphal structures such as perithecia and phialides, respectively. $\Delta Fgnot3$ mutants completely lost female fertility and failed to produce normal phialide cells, leading to markedly impaired spore production and abnormal conidium morphologies. The significant down-regulation of genes involved in conidiation, including *STUA*, *HTF1*, *REN1*, and *FLBC*, but not *ABAA* and *WETA*, supports the hypothesis that *FgNOT3* has global roles in asexual sporulation independent of the AbaA-WetA pathway. To our knowledge, this is the first report to implicate the contribution of Not3 homologs in both sexual and asexual developmental stages.

NOT3/5 mutations in yeasts affect cell wall structure. Therefore, the null mutants showed altered sensitivities to cell wall stress-inducing agents. Although $\Delta Canot5$ mutants of *C. albicans* are highly sensitive to Calcofluor white, they are more resistant to β -glucanase zymolyase than wild type [26]. $\Delta Scnot3$ mutants show increased sensitivity to caffeine in *S. cerevisiae* [52]. However, *FgNOT3* deletion mutants did not show any altered sensitivity to cell wall stress-inducing agents as well as other specific stresses as previously reported (data not shown) [9]. Intriguingly, we identified a novel function of *FgNOT3* in adaptation to thermal stress. Moreover, *FgNOT3* did not complement the *S. cerevisiae* $\Delta Scnot5$ mutant (S3 Fig). Differences in the function of Not3/5 in cell wall integrity between yeast and filamentous fungi may not only be derived from evolutionary divergence between the two groups but also might explain the diverse roles of Not3/5 in cellular processes among eukaryotes. CNot3 in mice is essential for multiple functions, including embryonic development and control of heart function, and the metabolism of adult mice supports this notion [28, 53].

Our transcript analyses provide some clues for understanding the interactions among the subunits of Ccr4-Not complex. Transcript levels of all Not subunits, including *FgNOT1*, *FgNOT2* and *FgNOT4*, were significantly altered, but those of other Ccr4-Not subunits were not, suggesting that they function within the context of the Not module. In addition, the transcript levels of *FgNOT1* and *FgNOT4* were decreased, whereas the *FgNOT2* transcript level was highly increased in the $\Delta Fgnot3$ compared to wild type for unknown reasons. Because the feedback regulation often occurs in protein complexes [54], FgNot2 might be a direct interactor of FgNot3 but not of FgNot1 and FgNot4. The heterodimerization of the Not module in the ScNot1-ScNot2-ScNot5 or CNot1-CNot2-CNot3 forms a platform for macromolecular interactions [55, 56]. While ScNot3/5 and ScNot2 seem to function together [16] and ScNot3 directly interacts with ScNot4 and ScNot5 in yeast [19, 24], there is no interaction between CNot3 and CNot4 in humans [47]. The interaction between these proteins in *F. graminearum* needs to be confirmed, but these differences might be attributed to a different composition of the complex or the evolutionary divergence in yeast, filamentous fungi, and human.

We further functionally characterized the Not module of the Ccr4-Not complex in *F. graminearum*. *FgNOT1* is an essential gene as reported in other eukaryotes [9]. $\Delta Fgnot2$ and $\Delta Fgnot4$ mutants had pleiotropic effects on phenotypes, including vegetative growth, sexual and asexual production, and virulence, similar to the impacts of $\Delta Fgnot3$, suggesting that the Not module composed of *FgNot1-4* is also conserved in *F. graminearum*. In yeast, the association of all Ccr4-Not subunits is essential for cell viability although it remains unclear whether each subunit functions only within the context of a complex or has distinct roles outside of the complex [16]. For example, ScNot4 mainly functions in the regulation of proteasome integrity, whereas the ScNot2-3/5 module has more fundamental roles. Therefore, $\Delta ScNot2$ and $\Delta ScNot5$ showed more pronounced growth defects than $\Delta ScNot4$ [16]. Consistently, *FgNOT4* deletion had a slight effect on phenotypes, but deletion of *FgNOT2* resulted in mostly indistinguishable phenotypic defects compared to $\Delta Fgnot3$ mutants.

FgNOT2, *FgNOT3*, and *FgNOT4* are negative regulators of ZEA and/or trichothecene production. Whereas $\Delta Fgnot2$ and $\Delta Fgnot4$ mutants produced significantly higher levels of ZEA and/or trichothecenes, $\Delta Fgnot3$ accumulated more than 40-fold higher levels of both ZEA and trichothecenes compared with wild type. The Not module of the Ccr4-Not complex appears to regulate upstream genes or transcriptional regulatory elements participating in the diverse regulation of multiple secondary metabolite biosynthetic clusters. Moreover, highly accumulated mycotoxins might affect the physiologies of the $\Delta Fgnot2$, $\Delta Fgnot3$, and $\Delta Fgnot4$ mutants. Although direct biological functions of mycotoxins have not been reported in *F. graminearum*, overproduction of secondary metabolites often leads to unexpected developmental defects. All of the 13 transcription factor mutants overproducing ZEA and/or trichothecenes show defective vegetative growth and/or reproduction [9], and *FgFlbA* deletion mutants accumulating both ZEA or trichothecenes at high levels also show pleiotropic defects in *F. graminearum* [57].

In summary, our study functionally characterized the Not3 subunit of the Ccr4-Not complex for the first time in filamentous fungi. *FgNOT3* is involved in hyphal morphogenesis and cellular differentiation, which are related to sexual and asexual sporulation as well as virulence in *F. graminearum*. In addition, we found that the Not module of the Ccr4-Not complex of *F. graminearum* is conserved and involved in numerous characteristics, including vegetative growth, reproduction, virulence, and secondary metabolism.

Supporting Information

S1 Fig. Targeted deletion and complementation of $\Delta Fgnot3$. (A) Strategies used for the deletion and complementation of $\Delta Fgnot3$. The 5'-flanking regions (black bars) of the *FgNOT3* ORF were used as probes for hybridization. WT, wild-type strain Z-3639; $\Delta Fgnot3$, *FgNOT3* deletion mutant; FgNot3c, $\Delta Fgnot3$ -derived strain complemented with *FgNOT3*; H, HindIII; P, PstI; GEN, geneticin resistance gene cassette; HYG, hygromycin B resistance gene cassette. (B) Southern blot analysis of the deletion and complementation of $\Delta Fgnot3$. Lane 1, wild-type strain Z-3639; lane 2, deletion mutant; lane 3, complementation strain. The sizes of DNA standards (kb) are indicated to the left of the blot.

(TIF)

S2 Fig. The mycelial morphology of $\Delta Fgnot3$ mutants on CM liquid medium. The mycelial morphology was observed on CM liquid medium after incubating for 8, 18, and 26 h. WT, wild-type strain Z-3639; $\Delta Fgnot3$, *FgNOT3* deletion mutant; FgNot3c, $\Delta Fgnot3$ -derived strain complemented with *FgNOT3*.

(TIF)

S3 Fig. Complementation assay of *FgNOT3* on *S. cerevisiae* Δ *Scnot5*. Cells were cultured for 3 days at 30°C at 200 rpm in SC lacking Ura (SC-Ura) and supplemented with ampicillin medium, harvested, and then diluted in distilled water. Aliquots of 10 μ l were point-inoculated on SC-Ura supplemented with ampicillin medium and incubated for 4 days at 30°C. Columns in each panel represent serial log dilutions. BY4741, *S. cerevisiae* wild-type strains BY4741 harboring plasmid pYES2; Δ *Scnot5*, *S. cerevisiae* deletion of *Scnot5* mutant harboring plasmid pYES2; Δ *Scnot5*::*FgNOT3*, *S. cerevisiae* Δ *Scnot5*-derived strain complemented with *F. graminearum* *FgNOT3*. (TIF)

S4 Fig. Targeted deletion and mutant complementation strategies for *FgNOT2* (A) and *FgNOT4* (B). The 5'-flanking regions (black bars) of *FgNOT2* ORF and *FgNOT4* ORF were used as probes for hybridization. WT, wild-type strain Z-3639; Δ *Fgnot2*, *FgNOT2* deletion mutant; *FgNot2c*, Δ *Fgnot2*-derived strain complemented with *FgNOT2*; Δ *Fgnot4*, *FgNOT4* deletion mutant; *FgNot4c*, Δ *Fgnot4*-derived strain complemented with *FgNOT4*; S, SacI; *GEN*, geneticin resistance gene cassette. Lane 1, wild-type strain Z-3639; lanes 2 and 3, deletion mutants; lanes 4 and 5, complementation strains. The sizes of DNA standards (kb) are indicated to the left of the blot. (TIF)

S1 Table. Primers used in this study.

(PDF)

Author Contributions

Conceived and designed the experiments: DCB HS YWL. Performed the experiments: DCB HS JYS HK. Analyzed the data: DCB HS JYS JCK HK GJC YWL. Contributed reagents/materials/analysis tools: HS JCK GJC YWL. Wrote the paper: DCB HS YWL.

References

- Goswami RS, Kistler HC. Heading for disaster: *Fusarium graminearum* on cereal crops. *Mol Plant Pathol.* 2004; 5: 515–525. doi: [10.1111/j.1364-3703.2004.00252.x](https://doi.org/10.1111/j.1364-3703.2004.00252.x) PMID: [20566626](https://pubmed.ncbi.nlm.nih.gov/20566626/)
- Sutton J. Epidemiology of wheat head blight and maize ear rot caused by *Fusarium graminearum*. *Can J Plant Pathol.* 1982; 4: 195–209.
- Desjardins AE. *Fusarium* mycotoxins: chemistry, genetics, and biology. St Paul, MN: American Phytopathological Society Press; 2006.
- Leslie JF, Summerell BA, Bullock S. The *Fusarium* laboratory manual. vol 10. Ames, IA: Blackwell Pub; 2006.
- Guenther JC, Trail F. The development and differentiation of *Gibberella zeae* (anamorph: *Fusarium graminearum*) during colonization of wheat. *Mycologia.* 2005; 97: 229–237. PMID: [16389974](https://pubmed.ncbi.nlm.nih.gov/16389974/)
- Lysoe E, Pasquali M, Breakspear A, Kistler HC. The transcription factor *FgStuAp* influences spore development, pathogenicity, and secondary metabolism in *Fusarium graminearum*. *Mol Plant Microbe Interact.* 2011; 24: 54–67. doi: [10.1094/MPMI-03-10-0075](https://doi.org/10.1094/MPMI-03-10-0075) PMID: [20879840](https://pubmed.ncbi.nlm.nih.gov/20879840/)
- Zheng W, Zhao X, Xie Q, Huang Q, Zhang C, Zhai H, et al. A conserved homeobox transcription factor Htf1 is required for phialide development and conidiogenesis in *Fusarium* species. *PLoS One.* 2012; 7: e45432. doi: [10.1371/journal.pone.0045432](https://doi.org/10.1371/journal.pone.0045432) PMID: [23029006](https://pubmed.ncbi.nlm.nih.gov/23029006/)
- Ohara T, Inoue I, Namiki F, Kunoh H, Tsuge T. *REN1* is required for development of microconidia and macroconidia, but not of chlamyospores, in the plant pathogenic fungus *Fusarium oxysporum*. *Genetics.* 2004; 166: 113–124. PMID: [15020411](https://pubmed.ncbi.nlm.nih.gov/15020411/)
- Son H, Seo Y-S, Min K, Park AR, Lee J, Jin J-M, et al. A phenome-based functional analysis of transcription factors in the cereal head blight fungus, *Fusarium graminearum*. *PLoS Pathog.* 2011; 7: e1002310. doi: [10.1371/journal.ppat.1002310](https://doi.org/10.1371/journal.ppat.1002310) PMID: [22028654](https://pubmed.ncbi.nlm.nih.gov/22028654/)
- Son H, Kim M-G, Min K, Seo Y-S, Lim JY, Choi GJ, et al. AbaA regulates conidiogenesis in the ascomycete fungus *Fusarium graminearum*. *PLoS One.* 2013; 8: e72915. doi: [10.1371/journal.pone.0072915](https://doi.org/10.1371/journal.pone.0072915) PMID: [24039821](https://pubmed.ncbi.nlm.nih.gov/24039821/)

11. Son H, Kim M-G, Min K, Lim JY, Choi GJ, Kim J-C, et al. WetA is required for conidiogenesis and conidium maturation in the ascomycete fungus *Fusarium graminearum*. *Eukaryot Cell*. 2014; 13: 87–98. doi: [10.1128/EC.00220-13](https://doi.org/10.1128/EC.00220-13) PMID: [24186953](https://pubmed.ncbi.nlm.nih.gov/24186953/)
12. Collart MA, Panasenکو OO. The Ccr4–not complex. *Gene*. 2012; 492: 42–53. doi: [10.1016/j.gene.2011.09.033](https://doi.org/10.1016/j.gene.2011.09.033) PMID: [22027279](https://pubmed.ncbi.nlm.nih.gov/22027279/)
13. Miller JE, Reese JC. Ccr4–Not complex: the control freak of eukaryotic cells. *Crit Rev Biochem Mol Biol*. 2012; 47: 315–333. doi: [10.3109/10409238.2012.667214](https://doi.org/10.3109/10409238.2012.667214) PMID: [22416820](https://pubmed.ncbi.nlm.nih.gov/22416820/)
14. Collart MA. Global control of gene expression in yeast by the Ccr4–Not complex. *Gene*. 2003; 313: 1–16. PMID: [12957374](https://pubmed.ncbi.nlm.nih.gov/12957374/)
15. Goldstrohm AC, Wickens M. Multifunctional deadenylase complexes diversify mRNA control. *Nature Rev Mol Cell Biol*. 2008; 9: 337–344.
16. Collart MA, Panasenکو OO, Nikolaev SI. The Not3/5 subunit of the Ccr4–Not complex: a central regulator of gene expression that integrates signals between the cytoplasm and the nucleus in eukaryotic cells. *Cell Signal*. 2013; 25: 743–751. doi: [10.1016/j.cellsig.2012.12.018](https://doi.org/10.1016/j.cellsig.2012.12.018) PMID: [23280189](https://pubmed.ncbi.nlm.nih.gov/23280189/)
17. Maillet L, Tu C, Hong YK, Shuster EO, Collart MA. The essential function of Not1 lies within the Ccr4–Not complex. *J Mol Biol*. 2000; 303: 131–143. PMID: [11023781](https://pubmed.ncbi.nlm.nih.gov/11023781/)
18. Bai Y, Salvadore C, Chiang Y-C, Collart MA, Liu H-Y, Denis CL. The *CCR4* and *CAF1* proteins of the *CCR4–NOT* complex are physically and functionally separated from *NOT2*, *NOT4*, and *NOT5*. *Mol Cell Biol*. 1999; 19: 6642–6651. PMID: [10490603](https://pubmed.ncbi.nlm.nih.gov/10490603/)
19. Collart MA, Struhl K. *NOT1* (*CDC39*), *NOT2* (*CDC36*), *NOT3*, and *NOT4* encode a global-negative regulator of transcription that differentially affects TATA-element utilization. *Genes Dev*. 1994; 8: 525–537. PMID: [7926748](https://pubmed.ncbi.nlm.nih.gov/7926748/)
20. Denis CL. Identification of new genes involved in the regulation of yeast alcohol dehydrogenase II. *Genetics*. 1984; 108: 833–844. PMID: [6392016](https://pubmed.ncbi.nlm.nih.gov/6392016/)
21. Draper MP, Salvadore C, Denis CL. Identification of a mouse protein whose homolog in *Saccharomyces cerevisiae* is a component of the CCR4 transcriptional regulatory complex. *Mol Cell Biol*. 1995; 15: 3487–3495. PMID: [7791755](https://pubmed.ncbi.nlm.nih.gov/7791755/)
22. Chen J, Rappsilber J, Chiang Y-C, Russell P, Mann M, Denis CL. Purification and characterization of the 1.0 MDa CCR4–NOT complex identifies two novel components of the complex. *J Mol Biol*. 2001; 314: 683–694. PMID: [11733989](https://pubmed.ncbi.nlm.nih.gov/11733989/)
23. Collart MA, Timmers H. The eukaryotic Ccr4–Not complex: a regulatory platform integrating mRNA metabolism with cellular signaling pathways? *Prog Nucleic Acid Res Mol Biol*. 2004; 77: 289–322. PMID: [15196896](https://pubmed.ncbi.nlm.nih.gov/15196896/)
24. Oberholzer U, Collart M. Characterization of *NOT5* that encodes a new component of the Not protein complex. *Gene*. 1998; 207: 61–69. PMID: [9511744](https://pubmed.ncbi.nlm.nih.gov/9511744/)
25. Villanyi Z, Ribaud V, Kassem S, Panasenکو OO, Pahi Z, Gupta I, et al. The Not5 subunit of the Ccr4–Not complex connects transcription and translation. *PLoS Genet*. 2014; 10: e1004569. doi: [10.1371/journal.pgen.1004569](https://doi.org/10.1371/journal.pgen.1004569) PMID: [25340856](https://pubmed.ncbi.nlm.nih.gov/25340856/)
26. Cheng S, Clancy CJ, Checkley MA, Zhang Z, Wozniak KL, Seshan KR, et al. The role of *Candida albicans* *NOT5* in virulence depends upon diverse host factors in vivo. *Infect Immun*. 2005; 73: 7190–7197. PMID: [16239513](https://pubmed.ncbi.nlm.nih.gov/16239513/)
27. Jin R, Dobry CJ, McCown PJ, Kumar A. Large-scale analysis of yeast filamentous growth by systematic gene disruption and overexpression. *Mol Biol Cell*. 2008; 19: 284–296. PMID: [17989363](https://pubmed.ncbi.nlm.nih.gov/17989363/)
28. Neely GG, Kuba K, Cammarato A, Isobe K, Amann S, Zhang L, et al. A global in vivo *Drosophila* RNAi screen identifies *NOT3* as a conserved regulator of heart function. *Cell*. 2010; 141: 142–153. doi: [10.1016/j.cell.2010.02.023](https://doi.org/10.1016/j.cell.2010.02.023) PMID: [20371351](https://pubmed.ncbi.nlm.nih.gov/20371351/)
29. Venturini G, Rose AM, Shah AZ, Bhattacharya SS, Rivolta C. *CNOT3* is a modifier of *PRPF31* mutations in retinitis pigmentosa with incomplete penetrance. *PLoS Genet*. 2012; 8: e1003040. doi: [10.1371/journal.pgen.1003040](https://doi.org/10.1371/journal.pgen.1003040) PMID: [23144630](https://pubmed.ncbi.nlm.nih.gov/23144630/)
30. Hu G, Kim J, Xu Q, Leng Y, Orkin SH, Elledge SJ. A genome-wide RNAi screen identifies a new transcriptional module required for self-renewal. *Genes Dev*. 2009; 23: 837–848. doi: [10.1101/gad.1769609](https://doi.org/10.1101/gad.1769609) PMID: [19339689](https://pubmed.ncbi.nlm.nih.gov/19339689/)
31. Bowden RL, Leslie JF. Sexual recombination in *Gibberella zeae*. *Phytopathology*. 1999; 89: 182–188. doi: [10.1094/PHYTO.1999.89.2.182](https://doi.org/10.1094/PHYTO.1999.89.2.182) PMID: [18944794](https://pubmed.ncbi.nlm.nih.gov/18944794/)
32. Harris SD. Morphogenesis in germinating *Fusarium graminearum* macroconidia. *Mycologia*. 2005; 97: 880–887. PMID: [16457357](https://pubmed.ncbi.nlm.nih.gov/16457357/)
33. Cappellini R, Peterson J. Macroconidium formation in submerged cultures by a non-sporulating strain of *Gibberella zeae*. *Mycologia*. 1965: 962–966.

34. Seo J-A, Kim J-C, Lee D-H, Lee Y-W. Variation in 8-ketotrichothecenes and zearalenone production by *Fusarium graminearum* isolates from corn and barley in Korea. *Mycopathologia*. 1996; 134: 31–37. doi: [10.1007/BF00437050](https://doi.org/10.1007/BF00437050) PMID: [20882466](https://pubmed.ncbi.nlm.nih.gov/20882466/)
35. Hong S-Y, So J, Lee J, Min K, Son H, Park C, et al. Functional analyses of two syntaxin-like SNARE genes, GzSYN1 and GzSYN2, in the ascomycete *Gibberella zeae*. *Fungal Genet Biol*. 2010; 47: 364–372. doi: [10.1016/j.fgb.2010.01.005](https://doi.org/10.1016/j.fgb.2010.01.005) PMID: [20102747](https://pubmed.ncbi.nlm.nih.gov/20102747/)
36. Sambrook J, Russell DW. *Molecular cloning: a laboratory manual*. 3rd ed. Cold Spring Harbor, NY: Cold Spring Harbor Laboratory Press; 2001.
37. Min K, Son H, Lee J, Choi GJ, Kim J-C, Lee Y-W. Peroxisome function is required for virulence and survival of *Fusarium graminearum*. *Mol Plant Microbe Interact*. 2012; 25: 1617–1627. doi: [10.1094/MPMI-06-12-0149-R](https://doi.org/10.1094/MPMI-06-12-0149-R) PMID: [22913493](https://pubmed.ncbi.nlm.nih.gov/22913493/)
38. Yu J-H, Hamari Z, Han K-H, Seo J-A, Reyes-Domínguez Y, Scazzocchio C. Double-joint PCR: a PCR-based molecular tool for gene manipulations in filamentous fungi. *Fungal Genet Biol*. 2004; 41: 973–981. PMID: [15465386](https://pubmed.ncbi.nlm.nih.gov/15465386/)
39. Han YK, Kim MD, Lee SH, Yun SH, Lee YW. A novel F-box protein involved in sexual development and pathogenesis in *Gibberella zeae*. *Mol Microbiol*. 2007; 63: 768–779. PMID: [17302802](https://pubmed.ncbi.nlm.nih.gov/17302802/)
40. Son H, Lee J, Park AR, Lee Y-W. ATP citrate lyase is required for normal sexual and asexual development in *Gibberella zeae*. *Fungal Genet Biol*. 2011; 48: 408–417. doi: [10.1016/j.fgb.2011.01.002](https://doi.org/10.1016/j.fgb.2011.01.002) PMID: [21237280](https://pubmed.ncbi.nlm.nih.gov/21237280/)
41. Kim H, Smith JE, Ridenour JB, Woloshuk CP, Bluhm BH. *HXK1* regulates carbon catabolism, sporulation, fumonisin B1 production and pathogenesis in *Fusarium verticillioides*. *Microbiology*. 2011; 157: 2658–2669. doi: [10.1099/mic.0.052506-0](https://doi.org/10.1099/mic.0.052506-0) PMID: [21719539](https://pubmed.ncbi.nlm.nih.gov/21719539/)
42. Jonkers W, Dong Y, Broz K, Kistler HC. The Wor1-like protein Fgp1 regulates pathogenicity, toxin synthesis and reproduction in the phytopathogenic fungus *Fusarium graminearum*. *PLoS Genet*. 2012; 8: e1002724.
43. Livak KJ, Schmittgen TD. Analysis of relative gene expression data using real-time quantitative PCR and the 2^{-ΔΔCT} method. *Methods*. 2001; 25: 402–408. PMID: [11846609](https://pubmed.ncbi.nlm.nih.gov/11846609/)
44. Gietz RD, Schiestl RH. Frozen competent yeast cells that can be transformed with high efficiency using the LiAc/SS carrier DNA/PEG method. *Nat Protoc*. 2007; 2: 1–4. PMID: [17401330](https://pubmed.ncbi.nlm.nih.gov/17401330/)
45. Szklarczyk D, Franceschini A, Kuhn M, Simonovic M, Roth A, Minguez P, et al. The STRING database in 2011: functional interaction networks of proteins, globally integrated and scored. *Nucleic Acids Res*. 2011; 39: D561–D568. doi: [10.1093/nar/gkq973](https://doi.org/10.1093/nar/gkq973) PMID: [21045058](https://pubmed.ncbi.nlm.nih.gov/21045058/)
46. Panepinto JC, Heinz E, Traven A. The cellular roles of Ccr4-NOT in model and pathogenic fungi—implications for fungal virulence. *Front Genet*. 2013; 4: 302. doi: [10.3389/fgene.2013.00302](https://doi.org/10.3389/fgene.2013.00302) PMID: [24391665](https://pubmed.ncbi.nlm.nih.gov/24391665/)
47. Albert TK, Lemaire M, van Berkum NL, Gentz R, Collart MA, Timmers HTM. Isolation and characterization of human orthologs of yeast CCR4–NOT complex subunits. *Nucleic Acids Res*. 2000; 28: 809–817. PMID: [10637334](https://pubmed.ncbi.nlm.nih.gov/10637334/)
48. Jiang J, Liu X, Yin Y, Ma Z. Involvement of a velvet protein FgVeA in the regulation of asexual development, lipid and secondary metabolisms and virulence in *Fusarium graminearum*. *PLoS One*. 2011; 6: e28291. doi: [10.1371/journal.pone.0028291](https://doi.org/10.1371/journal.pone.0028291) PMID: [22140571](https://pubmed.ncbi.nlm.nih.gov/22140571/)
49. Proctor RH, Hohn TM, McCormick SP. Reduced virulence of *Gibberella zeae* caused by disruption of a trichothecene toxin biosynthetic gene. *Mol Plant Microbe Interact*. 1995; 8: 593–601. PMID: [8589414](https://pubmed.ncbi.nlm.nih.gov/8589414/)
50. Jansen C, Von Wettstein D, Schäfer W, Kogel K-H, Felk A, Maier FJ. Infection patterns in barley and wheat spikes inoculated with wild-type and trichodiene synthase gene disrupted *Fusarium graminearum*. *Proc Natl Acad Sci USA*. 2005; 102: 16892–16897. PMID: [16263921](https://pubmed.ncbi.nlm.nih.gov/16263921/)
51. Boenisch MJ, Schäfer W. *Fusarium graminearum* forms mycotoxin producing infection structures on wheat. *BMC Plant Biol*. 2011; 11: 110. doi: [10.1186/1471-2229-11-110](https://doi.org/10.1186/1471-2229-11-110) PMID: [21798058](https://pubmed.ncbi.nlm.nih.gov/21798058/)
52. Kapitzky L, Beltrao P, Berens TJ, Gassner N, Zhou C, Wüster A, et al. Cross-species chemogenomic profiling reveals evolutionarily conserved drug mode of action. *Mol Syst Biol*. 2010; 6: 451. doi: [10.1038/msb.2010.107](https://doi.org/10.1038/msb.2010.107) PMID: [21179023](https://pubmed.ncbi.nlm.nih.gov/21179023/)
53. Morita M, Oike Y, Nagashima T, Kadomatsu T, Tabata M, Suzuki T, et al. Obesity resistance and increased hepatic expression of catabolism-related mRNAs in *Cnot3*^{+/-} mice. *EMBO J*. 2011; 30: 4678–4691. doi: [10.1038/emboj.2011.320](https://doi.org/10.1038/emboj.2011.320) PMID: [21897366](https://pubmed.ncbi.nlm.nih.gov/21897366/)
54. Yu J, Son H, Park AR, Lee S-H, Choi GJ, Kim J-C, et al. Functional characterization of sucrose non-fermenting 1 protein kinase complex genes in the Ascomycete *Fusarium graminearum*. *Curr Genet*. 2014; 60: 35–47. doi: [10.1007/s00294-013-0409-7](https://doi.org/10.1007/s00294-013-0409-7) PMID: [24057127](https://pubmed.ncbi.nlm.nih.gov/24057127/)

55. Bhaskar V, Roudko V, Basquin J, Sharma K, Urlaub H, Séraphin B, et al. Structure and RNA-binding properties of the Not1–Not2–Not5 module of the yeast Ccr4–Not complex. *Nature Struct Biol.* 2013; 20: 1281–1288.
56. Boland A, Chen Y, Raisch T, Jonas S, Kuzuoğlu-Öztürk D, Wohlbold L, et al. Structure and assembly of the *NOT* module of the human CCR4–NOT complex. *Nature Struct Biol.* 2013; 20: 1289–1297.
57. Park AR, Cho A-R, Seo J-A, Min K, Son H, Lee J, et al. Functional analyses of regulators of G protein signaling in *Gibberella zeae*. *Fungal Genet Biol.* 2012; 49: 511–520. doi: [10.1016/j.fgb.2012.05.006](https://doi.org/10.1016/j.fgb.2012.05.006) PMID: [22634273](https://pubmed.ncbi.nlm.nih.gov/22634273/)